

We are IntechOpen, the world's leading publisher of Open Access books Built by scientists, for scientists

6,900

Open access books available

185,000

International authors and editors

200M

Downloads

Our authors are among the

154

Countries delivered to

TOP 1%

most cited scientists

12.2%

Contributors from top 500 universities



WEB OF SCIENCE™

Selection of our books indexed in the Book Citation Index
in Web of Science™ Core Collection (BKCI)

Interested in publishing with us?
Contact book.department@intechopen.com

Numbers displayed above are based on latest data collected.
For more information visit www.intechopen.com



Hydrogen Fumigation on HD Diesel Engine: An Experimental and Numerical Study

Emad Monemian and Alasdair Cairns

Abstract

The currently reported work was concerned with experimental and numerical evaluation of the potential to partially replace diesel with hydrogen fuel, which continues to attract attention as an alternative longer-term fuel solution. The experimental work was involved with the fumigation of hydrogen on a single cylinder HD diesel engine under two real-world driving conditions at low and mid loads. Highest practical hydrogen substitution ratios could increase indicated efficiency by up to 4.6 and 2.4% while reducing CO₂ emissions by 58 and 32% at low and mid loads, respectively. Soot and CO emissions were reduced as more hydrogen was supplied, particularly at low load. The numerical study was made by using two distinct phenomenological models being run in parallel. While, an in-depth evaluation of the unique dual fuel combustion was possible, the arising errors were largely associated with lack of dual fuel burning velocity data, which will remain a key barrier to dual-fuel simulation.

Keywords: hydrogen, diesel, dual-fuel combustion, CO₂ reduction, simulation

1. Introduction

The climate change issue as the most obvious challenge of our era is threatening million lives around the world. Notwithstanding the treaties such as Kyoto [1] and Paris agreement [2] adopted during last decades to hinder the greenhouse gas (GHG) emissions, the promises were not kept fully due to rapid rate of industrialisation and trade races between countries. However, the recent environmental threats have gone off the alarm louder as several European countries have put deadlines to end urban utilisation of diesel engines. This call out could be carried out by gradual replacement of diesel fuel with alternative clean fuels like hydrogen particularly in the heavy goods vehicles (HGVs) as one of the main contributors of CO₂ emission.

Regarding the latest UK government target in 2019, GHG emissions will be cut to almost zero by 2050 within UK [3]. While the total CO₂ was reduced significantly (~30%) since the baseline year 1990 until 2014, the CO₂ emission in transport sector was almost unchanged representing 27.5% of total CO₂ in 2014 [4]. In that year, HGVs' CO₂ emission has experienced a 9% improvement compared with 1990. Despite the fact that UK is on track to meet the second "carbon budget" regarding the Climate Change Act 2008 [5], transport sector has not contributed

a major impact on CO₂ emission due to increase of motor vehicles sales in recent years [6]. As HGVs are accounted for 15.7% of UK transport sector's CO₂ emission, the vehicle manufacturers have been required to additionally focus upon Heavy Duty (HD) vehicles [4].

On the other hand, there is no economically viable single solution for HD long-haul applications and the internal combustion engine (ICE) is foreseen to remain as the key in the global marine, rail and continental truck markets albeit operating on lower carbon fuels. As HD diesel engine can hardly take advantage of the conventional measures applicable to the passenger car engine, it can be dual-fuelled with various fuels like natural gas (NG), ethanol, hydrogen, etc. Indeed, a pathway has been opened in recent years by the dual-fuel combustion to the sustainable operation of HD engines in the transport sector by significant reduction of CO₂ emission.

In this chapter, we aim to study the effect of substituting the diesel fuel with hydrogen in a HD diesel engine. Ameliorating the performance and decarbonisation of this engine is the main targets. Finally, a numerical study of H₂-diesel combustion was done in GT-Power.

2. Hydrogen usage in internal combustion engines

Hydrogen is conventionally seen being used as an energy carrier rather than fuel itself in ICEs. Typically, there are two main methods of supplying hydrogen: NG steam reforming (supplying ~95% of industrial H₂) and electrolysis of water (which is a zero-carbon method but very costly). Alternatively, an innovative acquirement of hydrogen is via on-board steam reformation of part of the liquid hydrocarbon fuel, which improves the overall system efficiency by ~5% via waste exhaust heat recovery [7]. Nevertheless, the vision of a “hydrogen economy” is only foreseeable when its required production energy is totally supplied from green renewable sources. If so, transportation and electrical needs can be fulfilled using hydrogen fuel cells [8].

Storage is among the main areas for development of hydrogen power due to the relevant safety issues and physical properties of hydrogen (**Table 1**). Although distinct crystalline materials have been suggested for hydrogen storage, hydrides are used for storing significant quantities of hydrogen gas. In 2008, a hydrogen tank using an alloy found by Robin Gremaud could have 60% less weight than a battery

Parameter	Hydrogen	Diesel
Density at 0°C [kg/m ³]	0.089	830
Stoichiometric air/fuel ratio	34.3	14.5
LHV [MJ/kg]	120	42.5
Mixture calorific value at $\lambda = 1$ [MJ/m ³]	3.2	3.83
Boiling temperature [°C]	-253	180–360
Ignition limits [vol%, λ]	4–75%, 0.2–10	0.6–5.5%, 0.5–1.3
Min ignition energy at air ($\lambda = 1$) [mJ]	0.02	0.24
Auto-ignition temperature [°C]	585	~250
Laminar flame speed at $\lambda = 1$ [m/s]	2.0	0.4–0.8
Carbon content (mass %)	0	86

Table 1.
Physical properties: hydrogen and diesel [9].

pack [10]. Besides, cryogenic tanks have other preferences which attempt to improve compatibility, expense and volumetric capacity. As an example of efforts in this area, BMW previously adopted cryogenic tanks for a 7-series mini-fleet to demonstrate improved driving range. The distribution of hydrogen for vehicles at filling stations needs remarkable infrastructure and huge investment. As of 2019, there are 46 public hydrogen stations in the US, with 41 of those located in California [11]. Thus, hydrogen would be a more sustainable fuel if its supplying and storage problems could be solved.

Several automotive manufacturers including BMW, Ford and Mazda have attempted to utilise hydrogen as an alternative fuel for the IC engine. The BMW Hydrogen 7, powered by a hydrogen IC engine, was developed by BMW between 2005 and 2007. This demonstrator adopted the same 6L V12 engine as the gasoline production model but with modifications to allow for dual fuel operation. Overall, the combustion system matched the efficiency values of a baseline turbo-diesel engine at a maximum of 42% [12].

Elsewhere, Ford also developed the first vehicle in North America exclusively powered by a hydrogen fuelled IC engine (H2ICE). A Zetec-based 2-liter H2ICE with a port fuel injection (PFI) system was integrated into a P2000 passenger sedan. Comparing with gasoline powered 2 L Zetec, hydrogen powered CO₂ emissions were reduced to 0.4% of that of the gasoline case with 18% higher metro cycle fuel economy [13]. In later work, to achieve the stringent 2010 Phase II Heavy Duty emission standards, Ford re-designed a V10 Triton engine with the aim of running an E-450 bus with hydrogen. Following this, the Ford Focus fuel cell vehicle (FCV) was developed as an alternative hydrogen fuel cell vehicle. Such FCV vehicles are widely considered to offer considerable promise but only provided the current high costs of fuel cell technology can be reduced in the longer term. Hence, in the medium term (at least), the ICE remains dominant [14].

There have been numerous other attempts to adopt hydrogen in IC engines. Revolve UK modified the engine of a Ford Transit 2.2L Puma Diesel to operate with PFI of hydrogen as the main fuel. As the ignition source, diesel pilot injection was used to allow a permanent dual-fuel mode [15]. More recently, Alset developed a hybrid hydrogen-gasoline system that allowed the vehicle to use both fuels individually or at the same time. This technology was implemented on the Aston Martin Rapide S, which was the first vehicle completing the 24-h Nürburgring race with hydrogen technology [16].

The injection strategy has considerable influence on the hydrogen mixture's homogeneity and stratification at ignition. Hydrogen direct injection (DI) could have further benefits rather than PFI due to providing more volumetric efficiency and avoiding irregular combustion such as backfire [17].

Lund university researchers have had the earliest attempt of hydrogen HCCI combustion [18]. Although H₂ HCCI operating range is much limited than SI hydrogen operation, HCCI mode showed better efficiency. In an optical study by Aleiferis et al. at UCL, hydrogen HCCI combustion was characterised by sweeping various equivalent ratios and intake air temperatures [19]. This combustion was initiated by PFI of n-heptane prior to the main DI of hydrogen in a low compression ratio combustion chamber. The intake air needed to be preheated as the auto-ignition temperature of hydrogen is too high. Considering significant ability of hindering CO₂ and nitrogen oxides (NO_x) intensely, the ideal zero emission engine can be realised as a rival to the fuel cell.

The unique physical properties of hydrogen make it quite different from conventional fuels, as indicated in **Table 1**. Due to the very low density, hydrogen's volumetric energy density is small relative to that of diesel even in a compressed storage tank or in liquid state. Hence, a large volume is needed for storing sufficient

hydrogen to perform a requisite driving range [20]. This fact highlights the benefits of hydrogen production through on-board reformation. According to **Table 1**, vast ignition limits (4–75% volumetric concentration in air), enables combustion over a wide domain of fuel-air mixtures including high efficiency lean operation. Furthermore, hydrogen has a relatively high flame speed that leads to higher efficiency [21].

Hydrogen's high diffusivity facilitates forming a uniform fuel-air mixture readily. This is also advantageous in the case of a hydrogen gas leakage, with rapid dispersion [20]. Low ignition energy of hydrogen and high burning speed makes the mixture of diesel/hydrogen easier to ignite, hence, mitigating misfire and improving performance and emissions. Besides, by increasing the H/C ratio, hydrogen enhances the mixture's energy density at lean mixtures. However, the full load must be supplemented by some means of volumetric efficiency compensation, such as compound boosting [20].

Comparing with diesel, hydrogen has meaningfully higher specific energy by mass, lower heating value (LHV), enabling a significant proportion of required diesel fuel be substituted by hydrogen in a more cost-effective way. However, diverse challenges remained are including high in-cylinder pressure rise rates and the occurrence of pre-ignition and flashback within the intake system, particularly under heavy loads. The high flame speed of hydrogen is favourable in terms of knock [20]. However, in-cylinder hotspots exposed during the intake stroke can serve as ignition sources for causing pre-ignition and flashback due to hydrogen's very low ignition energy. In addition, lubricant deposits or the sparkplug electrodes are also thought to initiate flashback [20].

3. Dual-fuel diesel combustion

Dual-fuel engine operation relies on method of introducing gaseous fuel which is hydrogen in our work. The conventional approach is adding gaseous fuel into the intake air flow like SI engines. The enrichment can also be done at start of compression stroke allowing fuel gas be mixed with air before diesel injection. Both these ways can be named as premixed dual-fuel engines with fumigation mode of enrichment. Other method of enrichment includes direct injection of fuel gas both whether prior to or after liquid fuel injection. In all approaches, gaseous fuel does not auto-ignite on its own via compression ignition, but usually burns with the assistance of the injected liquid-fuelled ignition processes [8].

In current work, fumigation of hydrogen into intake port of a heavy-duty diesel engine was applied, allowing a premixed dual-fuel combustion. The progress of conventional dual-fuel combustion (with diesel injection at near TDC), is depicted in **Figure 1**.

The complicated interaction of liquid fuel spray and bulk premixed gaseous fuel-air is not only thermal but has chemical kinetic feature which tends to extend the ignition delay and emissions. Thus, very precise control on timing of both fuel gas introduction and liquid fuel injection is essential [8].

Fuel type and concentration (in air) are important factors in premixed combustion as these parameters control chemical reaction rates. However, local flame velocity is affected heavily by mass and heat transfer. It is worthwhile to note that extra fuel or oxidant is needed for initiating burn process in partially premixed regions. These instances present complicated interaction among many chemical and physical reactions which are expressed on burn process in ICEs generally and in dual-fuel engines specifically. Chemical processes are generally governing in conditions relatively slower than physical mixing processes such as at low temperatures.

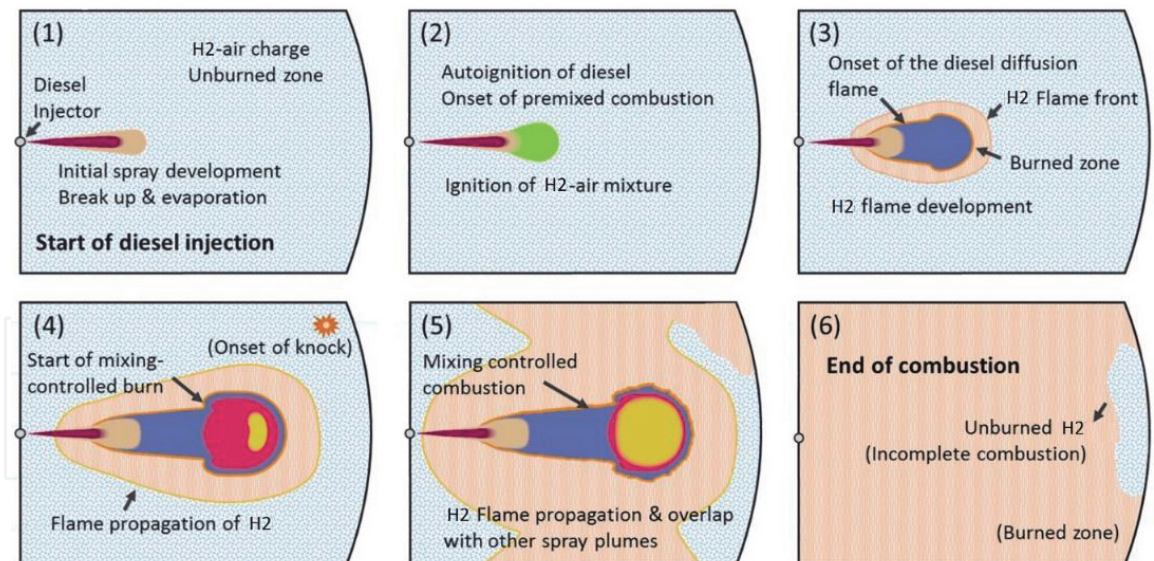


Figure 1.
 Progress of conventional H_2 -diesel dual-fuel combustion.

However, oxidation is altering exponentially on temperature which makes it happen more rapid than other physical processes. Sometimes for simplification, its effect on burn rate might be undermined or dismissed. Diffusion flame length requires to be regulated ensuring no extreme impingement and heat transfer would result in intolerable high temperature surfaces [8].

Fumigating gaseous fuel into intake air of a dual-fuel engine makes alteration in mixture's physical and transport properties such as specific heat ratio and heat transfer features. In addition, varying partial oxygen pressure resulted from gaseous fuel displacement, affects pre-ignition activity and its associated heat release which can be altered by residual gas effects. Therefore, ignition delay trend in dual-fuel engine is distinguished from conventional diesel engine. This delay extends with higher gaseous fuel fumigation up to a specified peak and later reduces to a value well before approaching the stoichiometric ratio based on combination of gaseous and liquid fuels with available air [8].

Some of the characteristics of dual-fuel combustion which make it more complicated than conventional SI and diesel combustion are as follows [8]:

- The gaseous fuel has low tendency to get oxidised completely at low loads which results in higher fuel consumption, HC and CO emissions.
- Since significant pre-ignition occurs sporadically within gaseous fuel-air mixture, fast heat release and pressure rise is observed.
- The knock threshold at high loads is characterised by uncontrolled auto-ignition and very fast partial combustion subsequently.

Mixing process within CI engines is important for leading combustion process properly. For instance, injecting low-amount pilot makes ignition occur after end of injection allowing mixture of pilot injected fuel with premixed gas fuel-air. Earlier pilot injection if not too early (pre-ignition), might start lean mixture combustion permitting more time for mixing of pilot with gas fuel.

It is worthwhile to mention that lower flammability limit (LFL) plays as a turning point in dual-fuel combustion as the mechanism is affected depending on which side of LFL, the hydrogen concentration is. To clarify this point, a conceptual

model proposed within a relevant work by [7] including the following three modes was considered:

1. When hydrogen concentration is above its LFL, hydrogen is pre-ignited resulting in an auto-ignition like homogeneous charge compression ignition (HCCI) mode or knocking combustion type.
2. In case of lean hydrogen (below LFL), hydrogen just burns in existence of diesel diffusion flame in a mixing-controlled mode.
3. If hydrogen concentration is over the LFL and in-cylinder conditions are not providing the hydrogen burn prior to diesel fuel ignition, the premixed hydrogen-air combustion develops in laminar mode encircling the diesel diffusion flame.

4. Experimental methodology

The test engine used for the experiments was an externally boosted single cylinder HD diesel engine which resembles the engine of a typical current European HGV, **Table 2**.

Supplying from a gas cylinder, hydrogen was fumigated downstream of the intake surge tank by mass flow controller. Gas detector and emergency shutdown circuit were embedded in the test cell with aim of protecting the operator and test facility against hydrogen leakage. In order to avoid risk of ignition in the intake system, a flashback arrestor was fitted to the hydrogen supply line, **Figure 2**.

As indicated in **Table 3**, two specific operating points were chosen for the hydrogen enrichment. The first corresponds to 1200 rpm and 6 bar net indicated mean effective pressure (IMEP_n), equivalent to 25% load representing operating point #7 of the ESC13 i.e. A25. The second operating point was 1200 rpm and 12 bar IMEP_n, equivalent to 50% load close to point #5 of the ESC13 i.e. A50.

Parameter	Value
Bore × stroke	129 × 155 mm
Connecting rod length	256 mm
Swept volume	2.026 dm ³
Number of valves	4
Compression ratio	16.8:1
Max in-cylinder pressure	180 bar
Diesel injection system	Bosch common rail, 220 MPa max injection pressure, 8 holes, 150° spray angle
Diesel fuel	Diesel-off-road “red” diesel (LHV = 42.9 MJ/kg)
Hydrogen enrichment	Continuous fumigation into intake port
Hydrogen material	BOC® CP grade hydrogen N5.0 (LHV = 120 MJ/kg)

Table 2.
Test engine specifications.

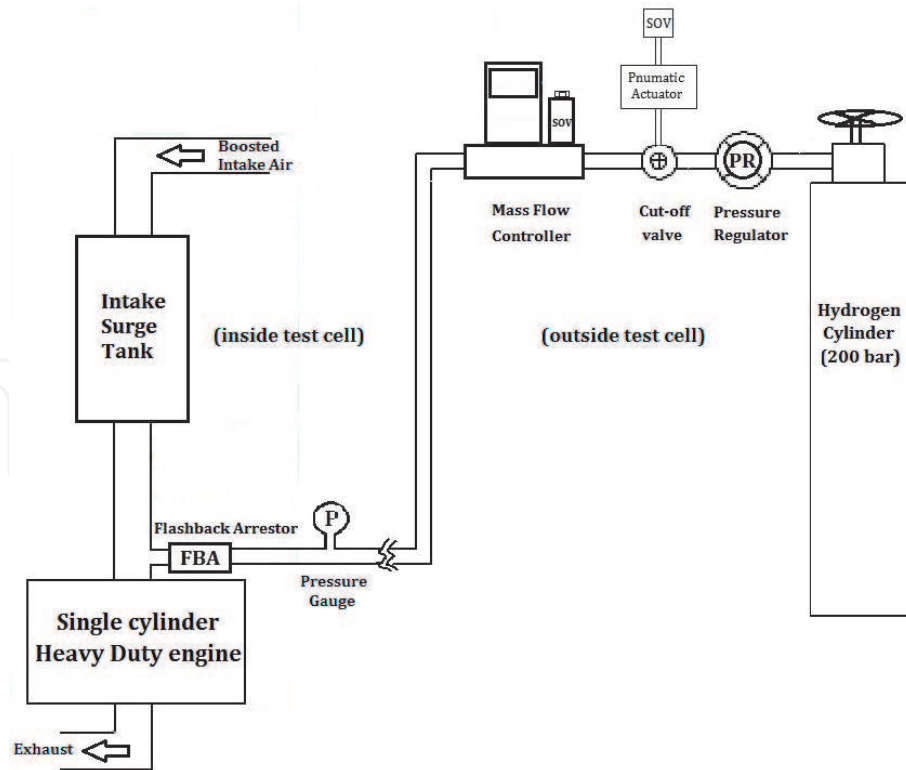


Figure 2.
 Experimental setup.

Parameter	Operating point 1 (A25)	Operating point 2 (A50)
Engine speed	1200 rpm	1200 rpm
Load (IMEPn)	6 bar	12 bar
Intake air temperature	309 K	318 K
Intake pressure	125 kPa	190 kPa
Exhaust pressure	135 kPa	200 kPa
EGR rate	25%	25%
EGR temperature	339 K	367 K
Rail pressure	1250 bar	1400 bar
Diesel injection strategy	Pre-injection	Pre-injection
H ₂ energy fraction range	0–65%	0–35%

Table 3.
 Engine operating conditions.

Based on energy input, the hydrogen fraction (HF) ratio was calculated, Eq. (1):

$$HF = \frac{\dot{m}_{hydrogen} LHV_{hydrogen}}{\dot{m}_{hydrogen} LHV_{hydrogen} + \dot{m}_{diesel} LHV_{diesel}} \times 100 \quad (1)$$

With aim of simplification in writing, it is convectional to use “H” plus a number to refer to a specific hydrogen fraction ratio (e.g. H20 means HF = 20%).

By optimising the start of injection (SOI) and its pressure, it was aimed to obtain the best indicated efficiency and indicated specific (IS) soot trade-off. While H₂ substitution ratio was altered with 10 and 5% increments at A25 and A50,

respectively; it is worthwhile to note that highest hydrogen fraction in each operating point, was limited by the maximum flow rate of H₂ mass flow controller (100 lit/min). Also, cyclic variation was defined by the coefficient of variation (COV) of the net IMEP averaged over 200 sampled cycles. The peak average pressure rise rate (PRR) and COV_{IMEPn} limits were set to 20 bar/deg and 5%, respectively.

5. Numerical methodology

GT-Power as a user-friendly and powerful engine simulation tool is used by many engine manufacturers and research centres. Based on one-dimensional fluid dynamics, flow and heat transfer are represented in all flow components of an engine unit. GT-Power is an object-oriented graphical user interface with robust modelling capabilities. This has minimised the input data amount since only specific geometrical elements are required. Hence, this commercial package was utilised for processing our numerical modelling of dual-fuel combustion using its phenomenological models.

The following assumptions are common for all of Gamma Technologies (GT) phenomenological models:

- The behaviours of all gases are assumed similar to that of the ideal gas.
- In whole engine cycle excluding combustion process (IVC to EVO), content of cylinder is assumed as a lump single-zone which is homogeneously mixed.
- The heat transfer between burned and unburned zones is neglected.
- Cylinder pressure is assumed uniform ($P_u = P_b = P_{cyl}$).
- Each zone has homogeneous temperature and chemical composition.
- The unburned zone composition is frozen and the composition of burned zone is kept in chemical equilibrium.

5.1 Three pressure analysis (TPA)

This section introduces the methodology of a reverse-run known as “three pressure analysis” (TPA) method for exploiting trapped in-cylinder condition and burn rate calculation. Regarding its name, this approach requires three measured pressures as inputs: in-cylinder, intake and exhaust. Thus, the corresponding engine model included valves and ports connected to a single cylinder crank case with all three required pressure curves versus crank angle degree (CAD) fed into it.

TPA approach is a multi-cycle simulation. For cycle 1, a mock burn rate is used with no pressure analysis. In next cycles, the forward-run will calculate the burn rate (Eq. (2)) using the trapped conditions at intake valve closure (IVC) and measured pressure profile at the start of each cycle. The injection profile and the heat transfer rate are imported from the previous cycle results. The burn rate will be iterated until the calculated cylinder pressure matches the measured cylinder pressure [22].

In the two-zone combustion model, the following energy equation is solved for the burned zone which determines burn rate $\left(\frac{dm_f}{dt}\right)$ [22]:

$$\frac{d(m_b e_b)}{dt} = -p \frac{dV_b}{dt} - Q_b - \left(\frac{dm_f}{dt} h_f + \frac{dm_a}{dt} h_a \right) \quad (2)$$

The main benefit of TPA is prediction of all of the cylinder trapped quantities particularly the residual fraction. Another benefit is providing the burn rate input data consistency check, as there is always some amount of error in calculation of burn rate from cylinder pressure due to sort of inaccuracies and/or assumptions in the model. All of these potential errors add to a single “cumulative error” which results in mismatching of the predicted burned fuel with total in-cylinder fuel mass. With aim of handling this problem, GT-POWER adjusts the fuel energy content (LHV) until the available fuel is consumed right at the end of the predicted burn rate. The amount of this fuel energy adjustment which is reported as “fuel energy (LHV) multiplier”, indicates the amount (and direction) of the cumulative error [22].

One of the beneficial results of TPA method is presenting a detailed energy analysis. As seen in **Figure 3**, the “in-cylinder energy balance” provides a comparison of following measured and predicted results thus can be used as a calibration tool:

- “Total fuel”
- “Burned fuel”
- “Cumulative energy” as the sum of internal energy, work and heat transfer.

5.2 GT “DIPulse” combustion model

In DIPulse model, the cylinder contents are divided into three thermodynamic zones including: the main unburned zone (all cylinder mass at IVC), the spray unburned zone (injected fuel and entrained gas) and the spray burned zone (combustion products). Using four calibration multipliers below, DIPulse is aimed to track the fuel as it was injected, evaporates and mixes with surrounding gas and burns. This model must be calibrated with experimental cylinder pressure analysis.

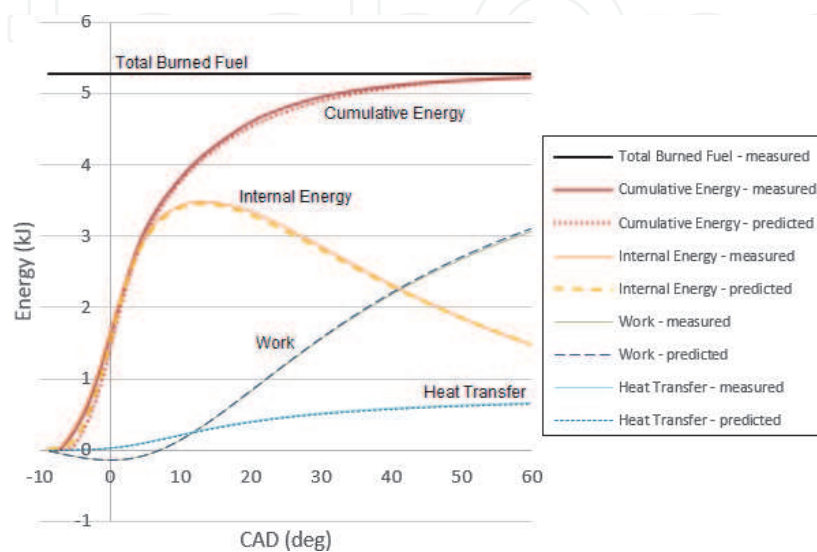


Figure 3.
 In-cylinder energy balance, HF = 15%.

Furthermore, in order to achieve acceptable correlation results, an absolute requirement is precise injection profiles for each test case:

- entrainment rate multiplier (entrain)
- ignition delay multiplier (igndelay)
- premixed combustion rate multiplier (premix)
- diffusion combustion rate multiplier (diff)

The physical processes during injection and combustion are simulated by several sub-models within DIPulse, as summarised in below flowchart (as the GT uses some proprietary equations for calculating these parameters, those are not mentioned here) (**Figure 4**):

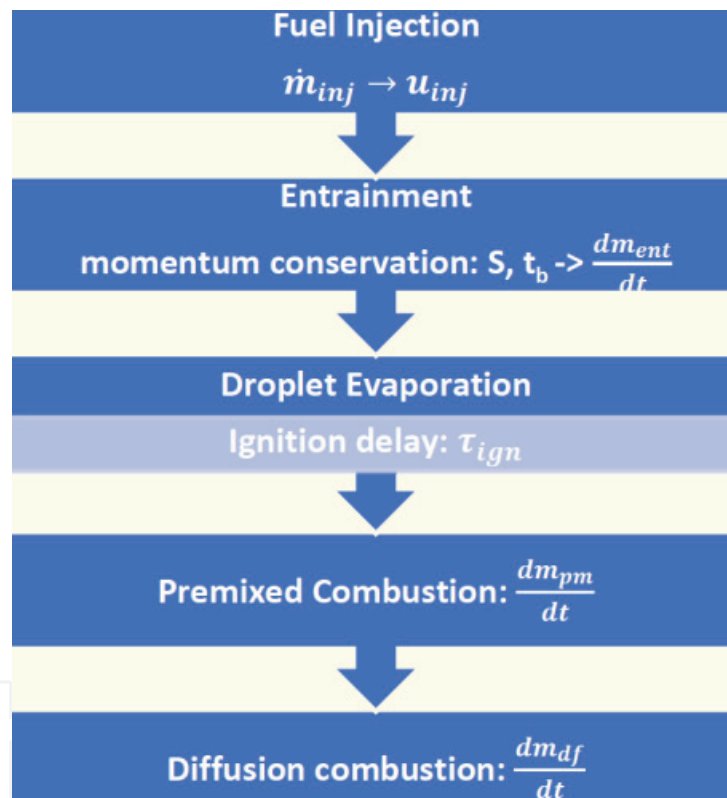


Figure 4. Flowchart of DIPulse calculations process.

5.3 GT “SITurb” combustion model

The rate of transferring the unburned gas into the flame front and converting to combustion products under laminar conditions is specified by laminar burning velocity (u_L). In laminar mode, the Taylor microscale (λ) is defined as the average distance of vortex sheets where the burn process takes place.

As the threshold velocity of combustion initiation, (unstretched) laminar burning velocity (u_L) has a dominance over whole combustion due to persisted interaction of initial combustion and charge motion. The laminar burning velocity is calculated by empirical correlations derived from pressure rise measured within constant-volume bombs or burners. Among those, the [23] correlation of “ u_L ” is

acknowledged to be the most comprehensive one incorporating the effects of unburned gas pressure, temperature, composition and residuals.

This correlation for various hydrocarbons and methanol and those at high pressure and temperatures can be fitted in form of a power law [24]:

$$u_L = u_{L,o} \left(\frac{T_u}{T_o} \right)^\alpha \left(\frac{P}{P_o} \right)^\beta \quad (3)$$

where $T_o = 298$ K and $P_o = 1$ atm are the reference temperature and pressure, and $u_{L,o}$, α and β are constants for a given fuel, equivalence ratio and burned gas diluent fraction. T_u is the temperature of unburned gas. For laminar burning velocity of hydrogen, the GT solver uses a proprietary equation similar to this equation with slight modification.

Since the turbulence parameters such as integral length scale (L), rms turbulent velocity (u') and laminar burning velocity (u_L) are difficult to measure experimentally under engine conditions, a numerical model must be used to estimate these parameters. The GT premixed combustion model, named as "SITurb" is based on the Blizzard and Keck model [25] which is the most applicable "turbulent entrainment model" used for SI engines [24]. The computational steps for this model are depicted in **Figure 5**:

This model is formed on three principle equations (Eqs. (4)–(6)) explained below. Regarding the fact that at the beginning, the flame is in laminar mode and then through the transition process which takes the time order of τ_b , it evolves to the turbulent flame, the burning law is defined [22]:

$$\tau_b = \frac{\lambda}{u_L} \quad (4)$$

The entrainment rate of unburned mass into the turbulent flame is given by [22]:

$$\frac{dM_e}{dt} = \rho_u A_{FF} u_{te} \quad (5)$$

M_e : entrained mass; ρ_u : unburned density; A_{FF} : flame front area; u_{te} : turbulent entrainment velocity.

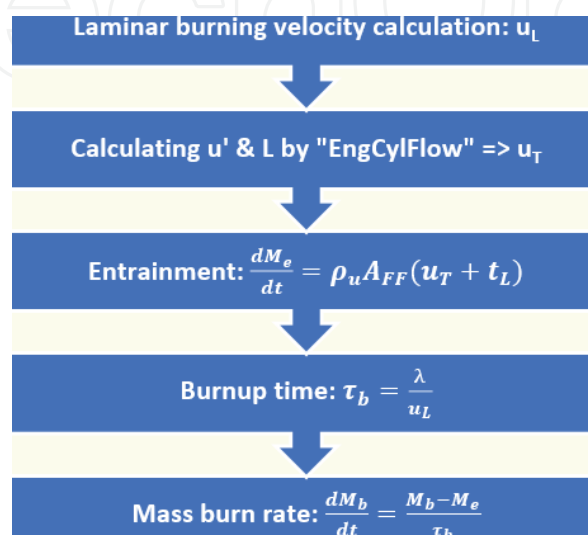


Figure 5.
 Flowchart of SITurb calculations process.

The rate of mass burning is determined as [22]:

$$\frac{dM_b}{dt} = \frac{M_e - M_b}{\tau_b} \quad (6)$$

where $(M_e - M_b)$ is the mass of entrained yet unburned gas and τ_b is the burning characteristic time defined in Eq. (4).

In GT-Power, the turbulent entrainment velocity in Eq. (4) has been replaced with $(u_T + u_L)$ in accordance with improvements applied to Keck and Blizzard model by Hires et al. [26]. This was aimed to split the effects of laminar burning velocity component normal to the flame surface and the turbulent distortion of flame surface.

By adjusting the effects of these parameters via three multipliers of SITurb model which are highlighted in red in the below equations, the premixed combustion can be calibrated [22]:

$$u_T = C_{TFS} u' \left(1 - \frac{1}{1 + C_{FKG} \left(\frac{R_f}{L} \right)^2} \right) \quad (7)$$

$$\lambda = \frac{C_{TLS} L}{\sqrt{Re_t}} \quad (8)$$

$$Re_t = \frac{\rho_u u' L}{\mu_u} \quad (9)$$

C_{TFS} : turbulent flame speed multiplier; Re_t : turbulent Reynolds number; C_{TLS} : Taylor length scale multiplier; μ_u : unburned zone dynamic viscosity; C_{FKG} : flame kernel growth multiplier; ρ_u : unburned density.

5.4 GT “DualFuel” combustion model

The conventional spark ignition models are not precisely applicable for premixed dual-fuel combustion particularly during the ignition and early stages of combustion as the pilot injection is applied. Indeed, the prospect model for dual-fuel combustion would divide the burn process into two dedicated regimes: pilot spray auto-ignition and the subsequent burning of premixed charge.

The “DualFuel” combustion model of GT-Power was used for predicting the burn rate for the dual-fuel engines where a pilot injection was used to ignite a premixed gaseous fuel/air mixture. This model combines the two distinct combustion models of DIPulse and SITurb. In this model, DIPulse handles the burning of the direct injected fuel and any premixed fuel that is entrained by the fuel spray and SITurb will model the resulting flame propagation for the premixed mixture. Both these two models take effect in parallel with an interaction between them.

Regarding optical observations, at the beginning of combustion, the spray shaped flames are formed. Then the flame front propagates into the unburned zone and ultimately will dominate the whole combustion chamber. Although, the flame front area for SITurb will initially use the conical area of the spray from DIPulse but the flame will finally transit to a spherical flame. A linear transition function will model this transformation [27]:

$$A_{FF} = \left(1 - \frac{R_f}{l_{k0}} \right) A_{FF_jet} + \left(1 - \frac{R_f}{l_{k0}} \right) A_{FF_hemispherical} \quad (10)$$

The schematic of dual-fuel engine modeled in GT-Power is seen in **Figure 6**.

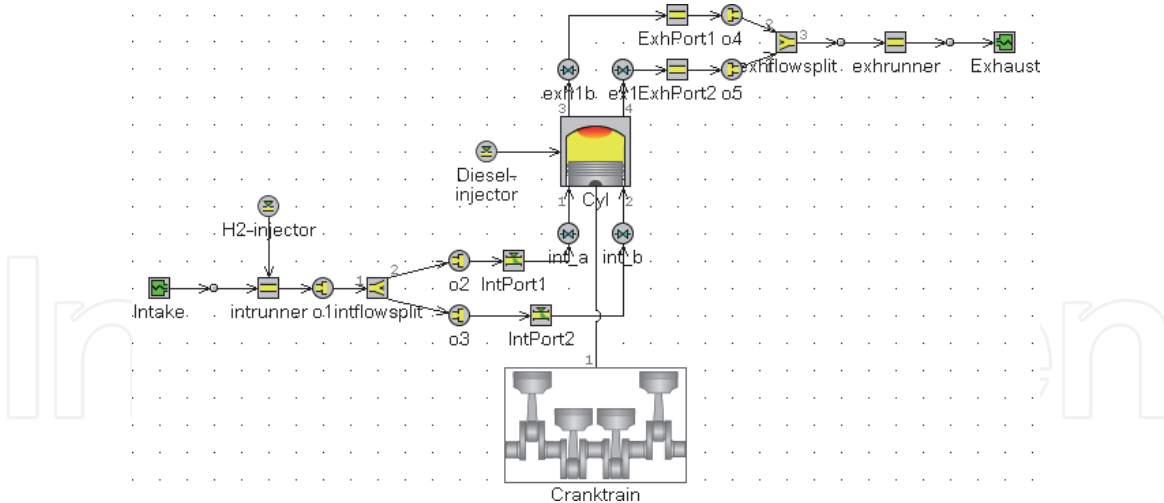


Figure 6.
 Schematic of dual-fuel engine model in GT-power.

6. Experimental results and analysis

6.1 H₂-diesel combustion analysis

According to the conceptual model proposed by [7] (explained at the end of Section 2), for experimental studying effect of hydrogen enrichment on diesel combustion, in each two operating points, specific hydrogen substitution ratios were selected regarding their H₂ concentration in air. Their corresponding burn rate

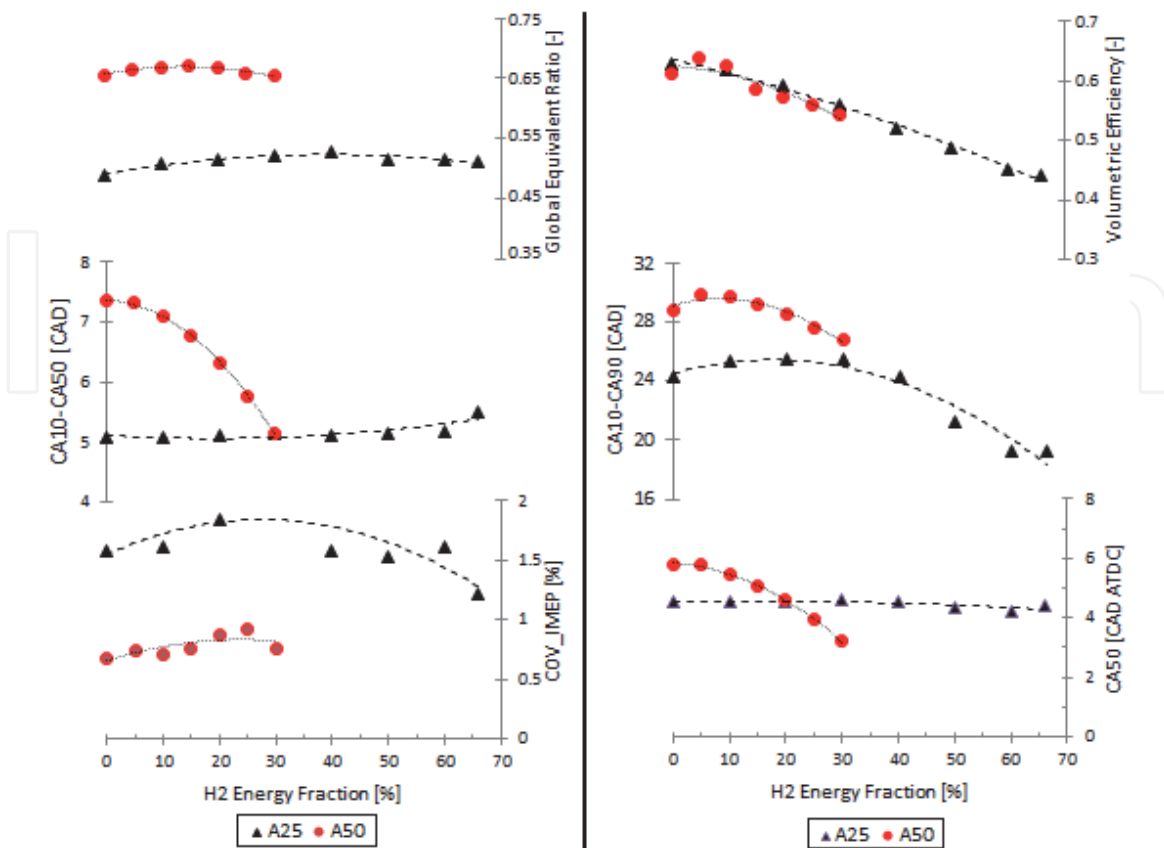


Figure 7.
 H₂-diesel: combustion characteristics [17].

and cylinder pressure plus the key attributes were post-processed by the TPA reverse-run calculation (explained in Section 5.1) on the measured test results. Four specific test cases chosen in the A25 operating point were: H0, H20, H40 and H65 and three ones chosen in the A50 were: H0, H15 and H30.

Combustion characteristics affected by hydrogen enrichment over two test operating points are presented in **Figure 7**. While ϕ_{global} was kept fairly constant for both loads, it was leaner at low load compared to mid load. Evaluating in-cylinder flow, it was observed that volumetric efficiency dropped drastically as expected. This is because significant amount of intake air was displaced with hydrogen which although has higher LHV but low molecular weight.

The key parameter, CA10-CA50, represents the premixed combustion part which set out and dominates the entire combustion process. While it was almost reluctant at A25, it was reducing monotonically by H₂ enrichment at A50. This phenomenon is felt well in burn rate comparisons presented in **Figure 8** as there is no variation at A25 while significant change is seemed at A50. The same trend was seen for combustion timing (CA50). These prove stimulating effect of hydrogen enrichment which was more pronounced at mid load in comparison to low load. In addition, as presented later, the flame radius and mass fraction burned for all selected cases at A25 except H65, are fairly reluctant to H₂ enrichment.

Nevertheless, combustion duration (CA10-CA90) was descending for both loads with shorter combustion for A25 cf. A50. A similar trend is reported in [28].

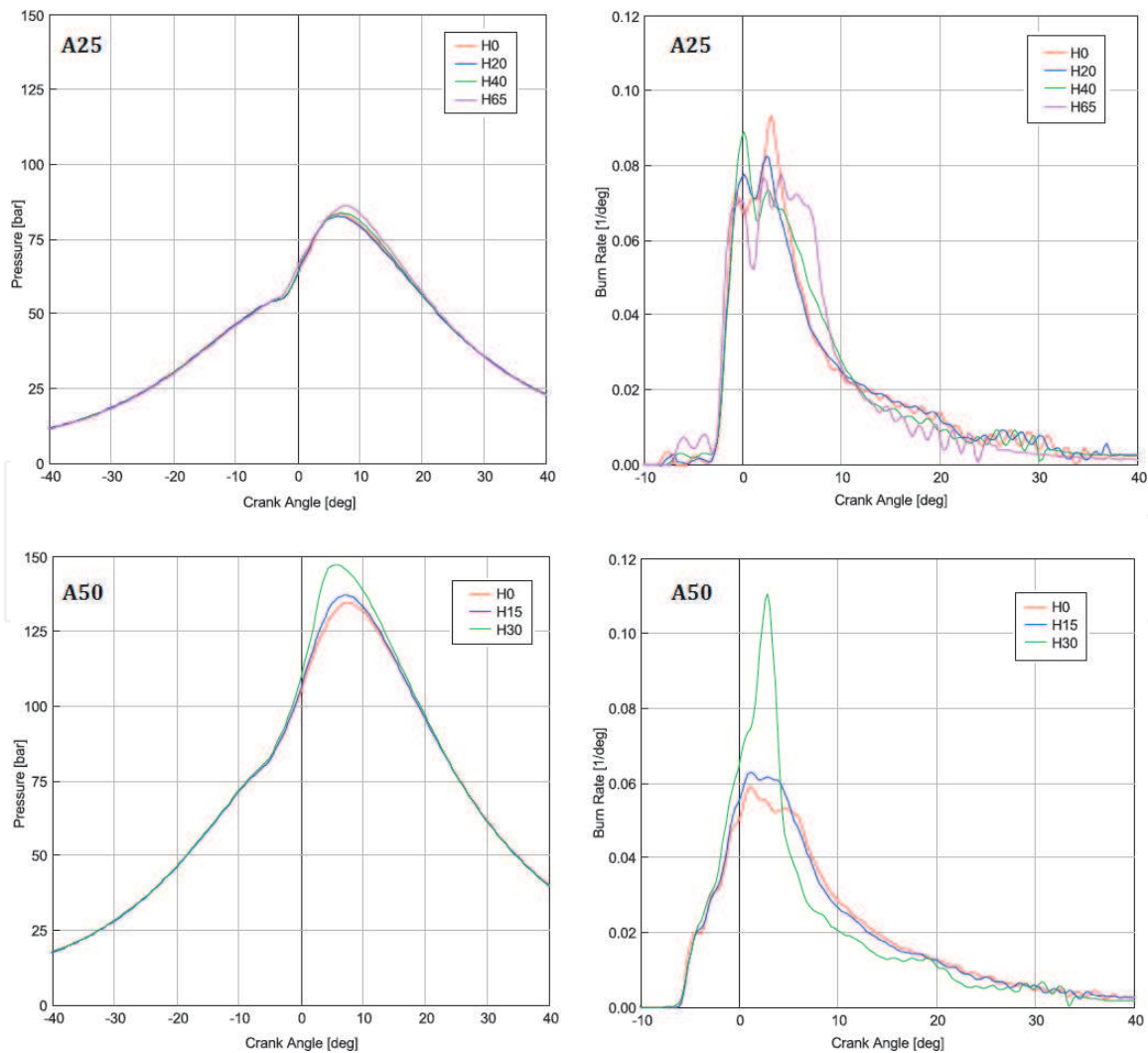


Figure 8. Cylinder pressure (left) and burn rate (right) for H₂-diesel dual-fuel combustion cases at A25 (top) and A50 (down).

Ultimately, despite higher cyclic variation at A50, the COV_IMEPn was slightly affected by HF change, resulted in reasonable COV (<5%) for both loads.

Despite the variations in key attributes of selected test cases, the cylinder pressure and burn rate trends are pretty similar for various HFs at A25. The reason can be related to low load characteristics which impede the hydrogen enrichment influence.

In contrast, the H₂ enrichment influence has evolved the combustion process for A50 cases. This claim is affirmed in **Figure 8** particularly for H30 where all key attributes were changed for both corresponding cylinder pressure and burn rate. Indeed, the mode 1 of the proposed conceptual model [7] is well presented in H30 whereas hydrogen pre-ignition prior to diesel fuel injection has been a game changer.

This phenomenon resulted in higher maximum pressure and PRR. In addition, combustion timing is advanced and burn duration is shortened significantly. More importantly, indicated efficiency has increased up to 46.44% i.e. 2.3% increase cf. H0 case, **Figure 9**. This is because less heat was transferred to cylinder wall due to faster combustion.

6.2 Exhaust emissions and performance of H₂-diesel combustion

Hydrogen enrichment had a positive effect on all carbon-related pollutants specially CO₂. According to **Figure 9**, ISSoot, ISCO and ISCO₂ all decreased abruptly by increasing HF for both loads due to reduction of the C/H ratio. This trend of dropping CO₂ emissions within dual-fuel HD diesel engine is very rewarding as the conventional HD diesel engines suffer from high CO₂ emission seriously.

On the other hand, nitrogen oxides emission rate increased with higher mass flow of hydrogen, as H₂ stimulates the combustion leading to higher temperatures.

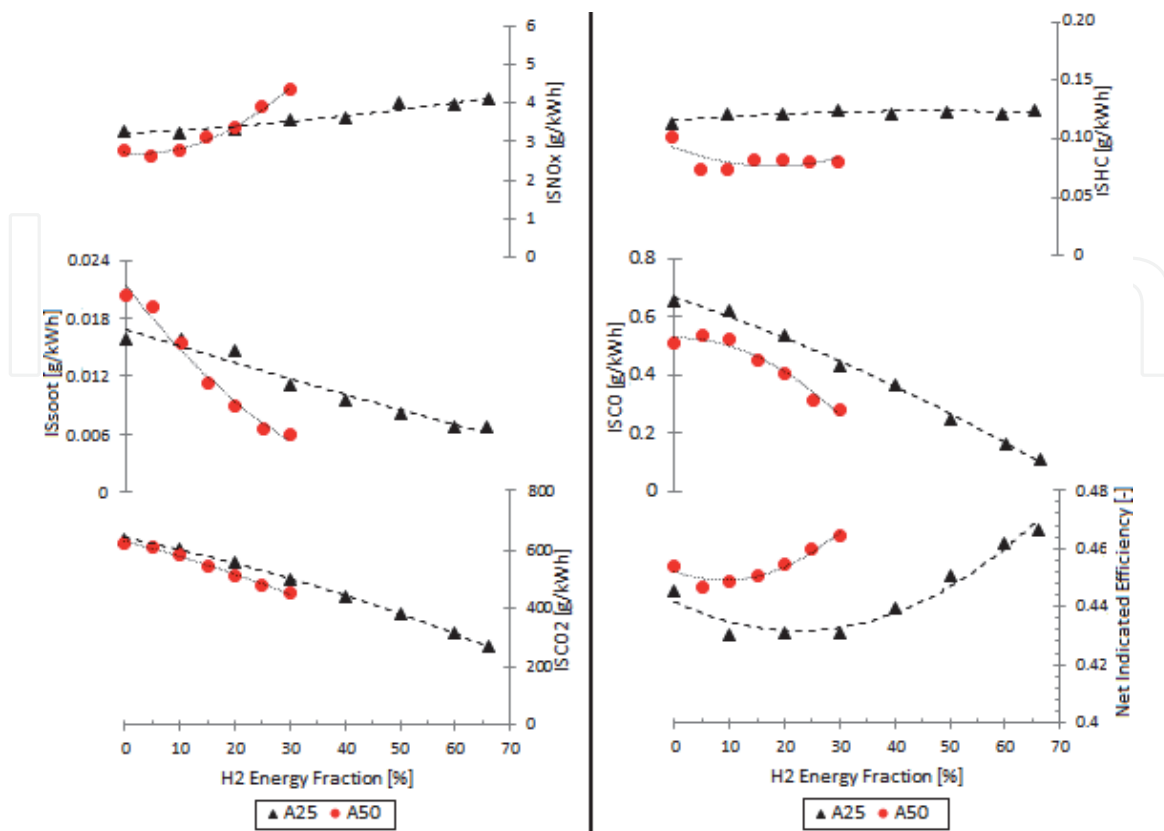


Figure 9. Exhaust emissions and performance (A25 and A50) [17].

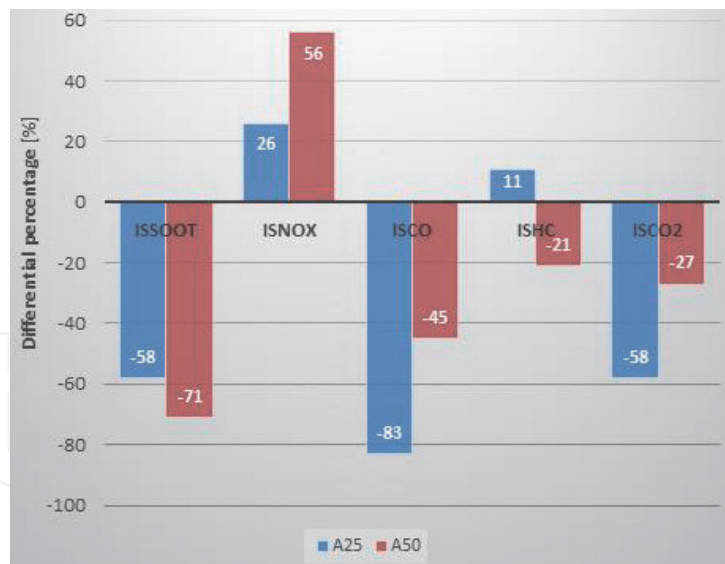


Figure 10.
Emissions alteration of highest HFs (H65 at A25 and H35 at A50) to diesel baseline.

NO_x- ϕ correlation presented in [29] can justify the ISNO_x trends presented in **Figure 9**. As average equivalence ratio at A25 was near NO_x rising threshold ($\phi = 0.5$), this resulted in relatively low increase of NO_x emission ($\sim 26\%$ c.f. diesel-only) in 6 bar IMEPn. However, the NO_x increase was significant at 12 bar IMEPn which exceeded 56% as the equivalence ratio was higher ($\phi = 0.66$) at A50. A same NO_x trend was observed by relevant work in [29].

One interesting characteristic with hydrogen fumigation was remaining the ISHC fairly reluctant, particularly at A25, where it was unchanged. This can be due to constant combustion timing.

Adding small amounts of hydrogen led to slight reduction in indicated efficiency, potentially associated with reduced ratio of specific heats due to displacement of air. The reason for initial drop in efficiency could be due to “hydrogen slip” (incomplete combustion of hydrogen) as claimed in [7]. This issue was more pronounced at low load as the diesel fuel injected was relatively small, hence the gaseous fuel could not fully burn by entraining into the liquid fuel. However, at higher substitution ratio the faster combustion of hydrogen outweighed this effect and led to improved efficiency especially after hydrogen’s lower flammability limit (LFL = 4% Vol). At A25, η_{ind} has a detrimental effect in the small hydrogen fractions until HF = 30%, where after efficiency starts to rise significantly until $\eta_{ind} = 46.5\%$. For A50, elevated η_{ind} starts to recover at HF = 10% and reaches a peak of 46.4% at the highest attainable HF.

The emission alteration for highest hydrogen fractions in two test points regarding the diesel-only baseline is presented in **Figure 10**.

7. H₂-diesel “dual-fuel” numerical analysis and results

Numerical analysis concludes the full assessment of the GT “DualFuel” modeling of measured H₂-diesel results considering the performance of the model. Initially, the multipliers of GT “DIPulse” and “SITurb” models were characterised using “Latin Hypercube” Design of Experiments (DOE) method within ranges recommended by GT. In association with TPA, the “Burn rate RMS” error can represent the error between the predictive burn rate and experimental burn rate measured by TPA. Our aim was minimising this error. With this aim, the threshold

of 0.005 was determined for the burn rate RMS which the values lower than that give acceptable burn rate correlation.

Following the DIPulse and SITurb characterisation, it was concluded the following influential multipliers for 'DualFuel' burn rate prediction in order of importance:

1. Diffusion multiplier
2. Entrainment multiplier
3. Turbulent flame speed multiplier
4. Ignition delay multiplier (featured by SOI)

Thus, it was attempted to achieve the best fit of dual-fuel model for simulating H₂-diesel combustion in the A25 as seen in **Figure 11**.

For overall evaluation of DualFuel model capability of simulating H₂-diesel combustion, the mass burned fraction (MBF) for the selected case at A25 were calculated. As seen in **Figure 12**, the rate of turbulent premixed combustion could not be predicted precisely. This is the result of a source of error which appeared mostly at the end of mass burning. The reasons for this source of error could include:

- De-developing turbulence is not taken into account in the SITurb model.
- The flame-wall interactions and associated physical phenomena are also not directly accounted for (i.e. quench).
- Considerable scatter in the burning velocity correlations.

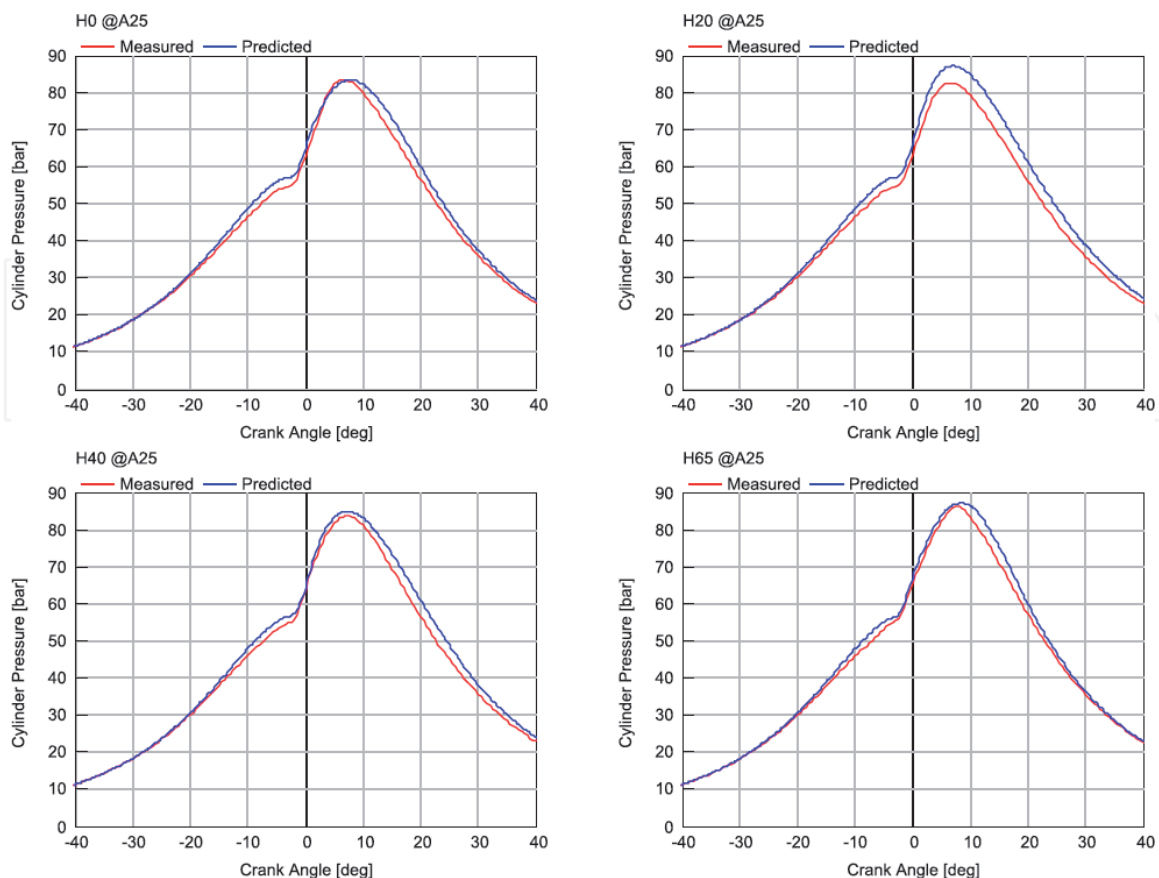


Figure 11.
Cylinder pressure prediction at A25.

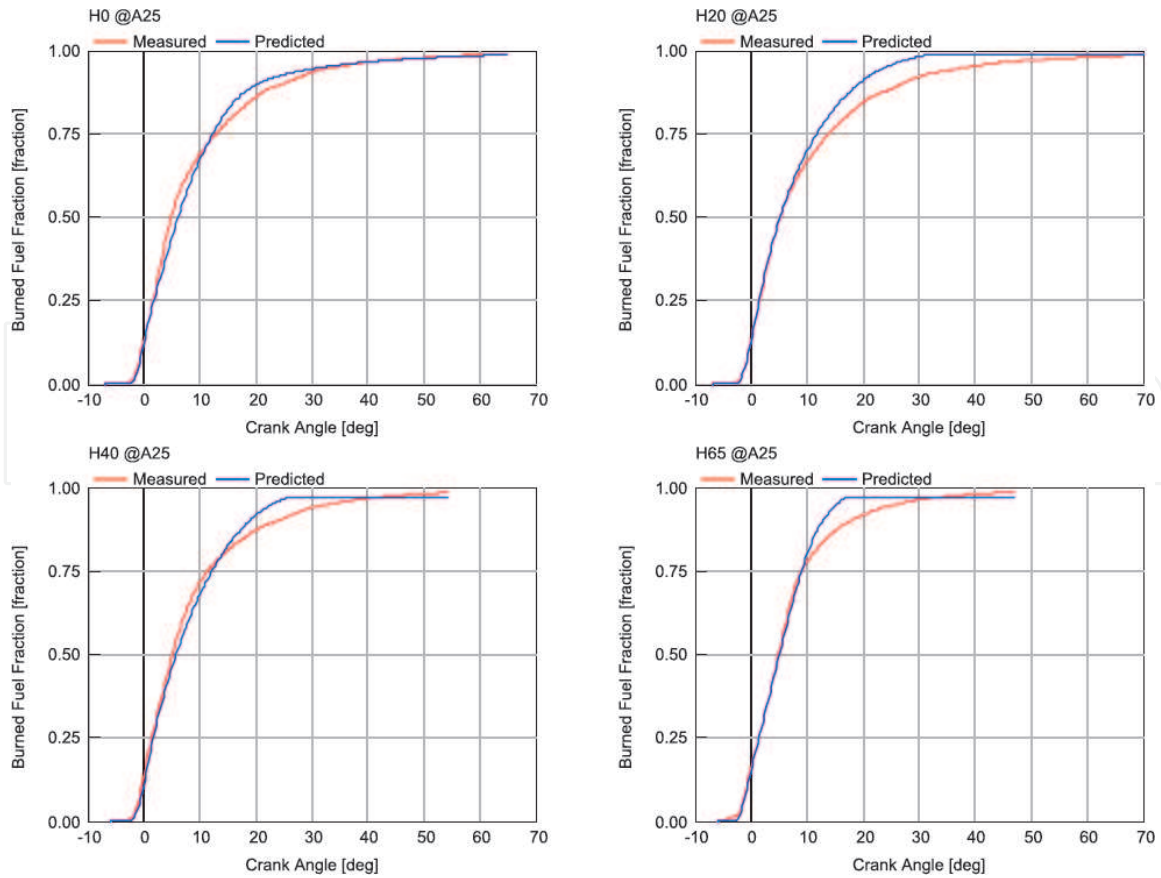


Figure 12.
 Mass burned fraction for selected cases at A25.

The empirical flame speed ratio (FSR) as ratio of turbulent flame speed to laminar flame speed, was employed in the DualFuel model in order to define the flame propagation rate. FSR usefully indicates if the combustion is most affected by chemical factors (laminar flame) or turbulence. Indeed, FSR is a useful metric for comparing the ability of the flow field to increase the rate of unburned mass entrainment.

As seen in **Figure 13**, both laminar and turbulent flame speeds were increased by enriching more hydrogen in the dual-fuel combustion mode. These changes are all explainable regarding the conceptual model proposed by [7], within which the hydrogen volumetric concentration in air has a key role in dual-fuel combustion of hydrogen and diesel. In fact, the hydrogen LFL plays as a turning point where exceeding this limit leads to hydrogen pre-ignition in the hydrogen/air premixed charge.

Despite the enhancement of flame speeds in both laminar and turbulent regimes for H65, this case has the lowest FSR comparing with other HFs, **Figure 13**. This can be interpreted that combustion process was mostly influenced by the laminar chemical reactions rather than turbulence. However, the combustion was shorter in this case than other HFs. In addition, **Figure 13** shows the highest FSR curve for H20 (lowest H₂ fraction). This represents that influence of turbulence was more robust than effect of the chemical reactions initiated the flame at earliest stage of combustion. Therefore, hydrogen enrichment contributed mostly in accelerating the early chemical reactions rather than enhancing the turbulence level.

As depicted in **Figure 14**, the significant rise of laminar flame speed for H65 is related to its extra-ordinary rise of the in-cylinder temperature (Eq. (3)). This significance can also be assessed by the specific heat ratio ($\gamma = \frac{c_p}{c_v}$) as the indicator

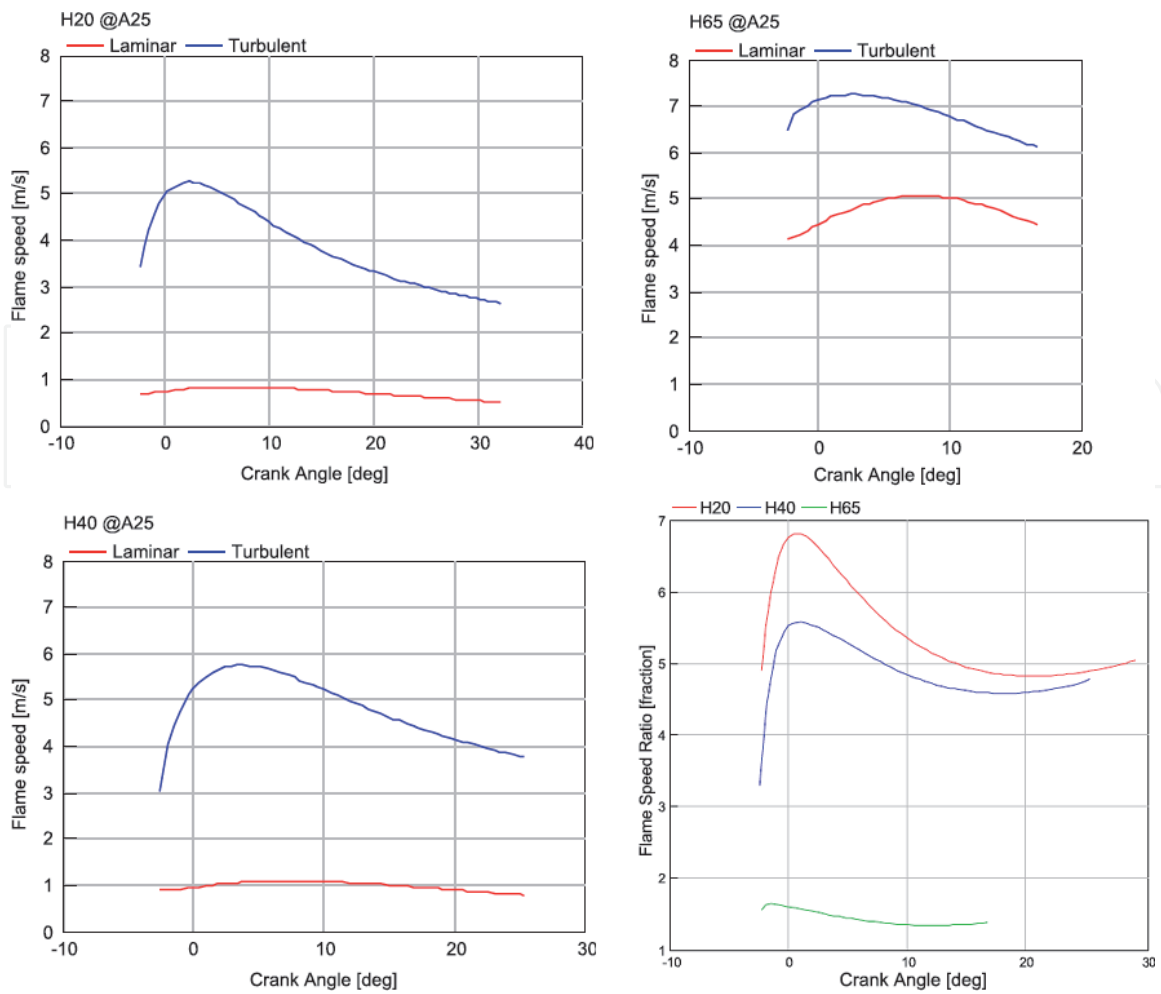


Figure 13.
 Flame speeds of selected test cases at A25.

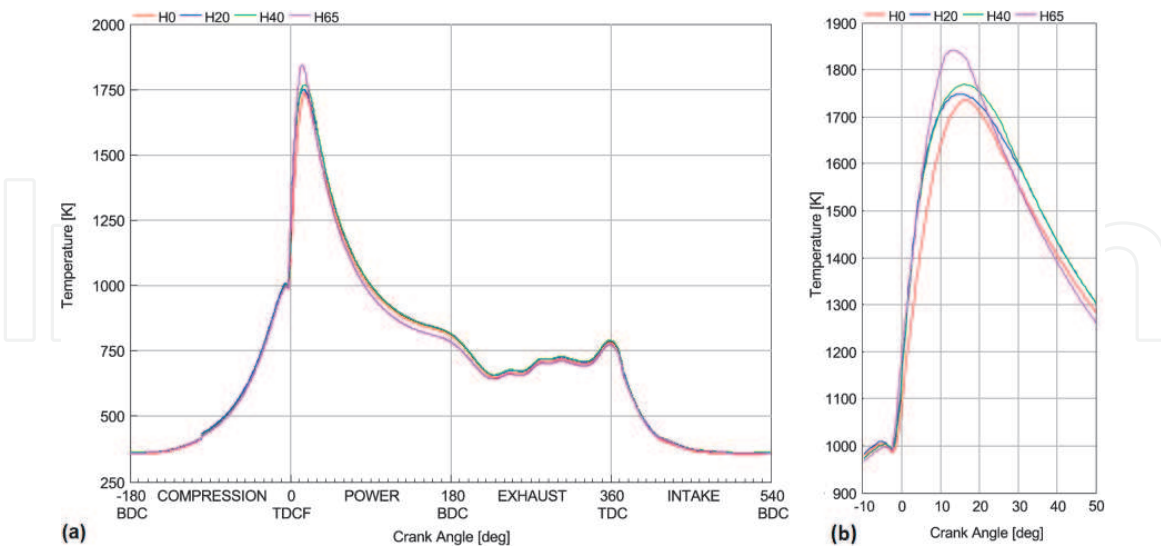


Figure 14.
 In-cylinder temperature during (a) entire cycle (b) combustion process at A25.

of sources of efficiency [24] during the engine cycle. As seen in **Figure 15**, this case has the highest γ over the engine cycle in comparison to other test cases. This can contribute in achieving the highest indicated efficiency among all HFs at A25, as depicted in **Figure 9**.

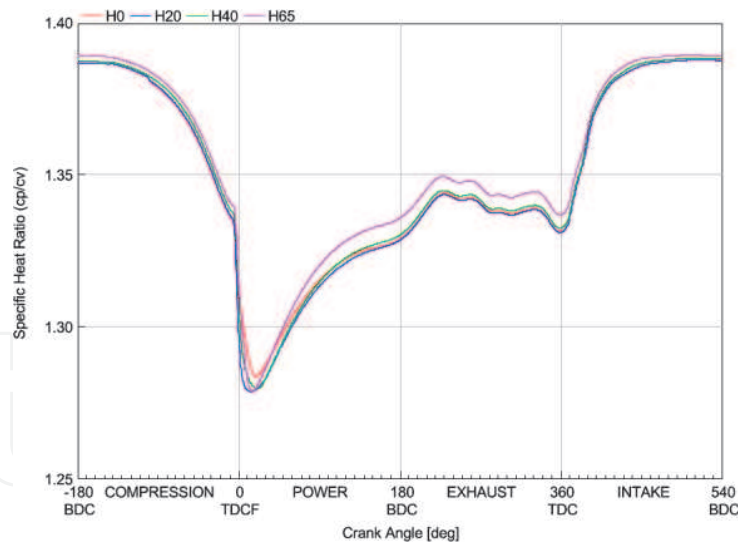


Figure 15.
Specific heat ratio at A25–DualFuel model.

8. Conclusions

8.1 Experimental tests conclusions

Comparing to the baseline diesel-only test results on our two targeted operating points (A25 and A50), it was aimed to achieve the best indicated efficiency-ISSoot trade-off. The following main points were concluded:

- Highest hydrogen substitution ratios increased indicated efficiency by up to 4.6% at 6 bar IMEPn and 2.4% at 12 bar IMEPn.
- ISCO₂, ISCO and ISSoot were reduced by 58, 83 and 58% respectively at 6 bar IMEPn. At 12 bar IMEPn, the reduction of these pollutants was 27, 45 and 71% respectively compared to the diesel-only baseline.
- H₂-diesel dual-fuel combustion with fixed SOI resulted in an increase of NO_x emissions (~26%) at 6 bar IMEPn. This increase was significant at 12 bar IMEPn, which exceeded 56%, but is an inherent feature of the elevated temperatures incurred. NO_x emission could meet the 0.4 g/kWh limit of Euro VI with NO_x after-treatment of 90% conversion efficiency.

8.2 Numerical study conclusions

For the first time, in the currently reported work, two distinct phenomenological sub-models, “DIPulse” and “SITurb” were run in parallel in the form of a DualFuel model, to simulate the H₂-diesel combustion. Although, the sub-models showed good capability of predicting the in-cylinder pressure, the DualFuel model suffers from insufficiencies in modelling of dual-fuel combustion particularly in high HFs. Despite its novelty, this current model may contain some pitfalls as follow:

- The model is in its infancy to be applied for dual-fuel modelling due to its oversimplified assumptions (e.g. single-zone homogeneous turbulence model with averagely-sized eddies).

- The model relies heavily on correlations to engine data (flame images, cylinder pressure and burn rate) to have an inclusive predictive performance.
- The laminar burning velocity correlation for hydrogen does not include the effects of flame instabilities which result in an apparent rise in u_L and hence pressure. Besides, the necessity of experimentally measuring the burning velocity of hydrogen within the premixed diesel charge is greatly acknowledged to allow us to have better insight of dual-fuel combustion physics. Although, this dual-fuel flame speed measurement has been mostly overlooked by fellow researchers, this can be very beneficial as premixing diesel could typically extend the lean burn limit with enhancing combustion efficiency of dual-fuel engines.
- The interaction between DIPulse and SITurb within DualFuel model is not yet known exactly in detail. Indeed, those might be able to predict the “trend” of combustion process rather than prediction of corresponding variables accurately.

Despite these barriers, the predictive model could be used for calculating the flame speeds (laminar and turbulent) in addition to other turbulent parameters for each test case. The results of our numerical study can be concluded as follow:

- The influential multipliers for ‘DualFuel’ burn rate prediction in order of importance are: diffusion, entrainment, turbulent flame speed and ignition delay.
- The laminar flame speed is increasing by enriching more hydrogen in dual-fuel combustion mode. This enhancement is more pronounced for highest HF (H65) as it is related to its extra-ordinary rise of the in-cylinder temperature.
- The H65, has the fastest flame propagation. This is in accordance with MFB curve of this case which resulted in shortest combustion duration among all cases. Nevertheless, H65 has the lowest FSR comparing with other HFs emphasising that its combustion process was mostly affected by the chemical activities rather than turbulence.
- The highest FSR was obtained by lowest HF (H20). Hence, hydrogen addition was mainly pronounced in expediting the early stage chemical reactions instead of turbulence level enhancement.
- As a proof for achieving the highest indicated efficiency by H65 at A25, the highest specific heat ratio was obtained by this test case over entire engine cycle.

Acknowledgements

The financial support of VN-Automotive Ltd. is acknowledged for commissioning the experimental work.

Conflict of interest

The authors declare there is no conflict of interest for publishing this chapter.

Acronyms

CAD	crank angle degree
COV	coefficient of variation
DI	direct injection
DOE	design of experiments
FCV	fuel cell vehicle
FSR	flame speed ratio
GHG	greenhouse gas
GT	Gamma Technologies®
H2ICE	hydrogen fuelled IC engine
HCCI	homogeneous charge compression ignition
HD	heavy duty
HF	hydrogen fraction
HGV	heavy goods vehicles
HRR	heat release rate
ICE	internal combustion engine
IMEP _n	net indicated mean effective pressure
IS	indicated specific
IVC	intake valve closure
LFL	lower flammability limit
LHV	lower heating value
MBF	mass burned fraction
NG	natural gas
NO _x	nitrogen oxides
PFI	port fuel injection
PRR	pressure rise rate
SOI	start of injection
TPA	three pressure analysis
UCL	University College London

IntechOpen

Author details

Emad Monemian* and Alasdair Cairns
University of Nottingham, Nottingham, UK

*Address all correspondence to: emad.monemian@gmail.com

IntechOpen

© 2020 The Author(s). Licensee IntechOpen. Distributed under the terms of the Creative Commons Attribution - NonCommercial 4.0 License (<https://creativecommons.org/licenses/by-nc/4.0/>), which permits use, distribution and reproduction for non-commercial purposes, provided the original is properly cited. 

References

- [1] Kyoto Protocol. Available from: https://en.wikipedia.org/wiki/Kyoto_Protocol [Accessed: 15 August 2019]
- [2] Adoption of the Paris Agreement, United Nations, Framework Convention on Climate Change, UN Doc FCCC/CP/2015/L.9/Rev.1 [Adopted: 12 December 2015]
- [3] Climate Change: UK Government to Commit to 2050 Target. BBC News. Available from: <https://www.bbc.co.uk/news/science-environment-48596775> [Released: 2019-06-19]
- [4] Final UK Greenhouse Gas Emissions National Statistics 1990-2014. Available from: https://assets.publishing.service.gov.uk/government/uploads/system/uploads/attachment_data/file/496946/2014_Final_Emissions_Statistical_Summary_Infographic.pdf [Accessed: 15 August 2019]
- [5] Climate Change Act 2008. Available from: http://www.legislation.gov.uk/ukpga/2008/27/pdfs/ukpga_20080027_en.pdf [Accessed: 15 August 2019]
- [6] Provisional New CV Registrations or Sales (2014), OICA statistics. Available from: <http://www.oica.net/category/sales-statistics/> [Accessed: 10 July 2017]
- [7] Morgan R, Atkins P, Atkins A, Lenartowicz C, Heikal M. Effect of Hydrogen Fumigation in a Dual Fueled Heavy Duty Engine. SAE Technical Paper 2015-24-2457. 2015
- [8] Karim GA. Dual-Fuel Diesel Engines. Boca Raton: CRC Press; 2015
- [9] Wimmer A, Wallner T, Ringler J, Gerbig F. H₂-Direct Injection—A Highly Promising Combustion Concept. SAE Technical Paper, 2005-01-0108. 2005
- [10] Light Weight Hydrogen ‘Tank’ Could Fuel Hydrogen Economy, Science Daily. Available from: <https://www.sciencedaily.com/releases/2008/11/081104084215.htm> [Released: 5 November 2008]
- [11] Alternative Fueling Station Counts by State, Alternative Fuels Data Center, US Dept. of Environment. Available from: https://www.afdc.energy.gov/fuels/stations_counts.html [Retrieved: 15 August 2019]
- [12] BMW Hydrogen 7. Available from: http://en.wikipedia.org/wiki/BMW_Hydrogen_7 [Accessed: 15 August 2019]
- [13] Szwabowski SJ, Hashemi S, Stockhausen WF, et al. Ford Hydrogen Engine Powered P2000 Vehicle. SAE Technical Paper 2002-01-0243. 2002
- [14] Natkin RJ, Denlinger AR, Younkins MA, et al. Ford 6.8L Hydrogen IC Engine for the E-450 Shuttle Van. SAE Technical Paper 2007-01-4096. 2007
- [15] Low Carbon Vehicle Partnership. Innovations in UK road transport: Driving the economy, cutting carbon [Reported: 9 March 2015]
- [16] Alset Global “Our Solutions”. Available from: <http://alset.at/our-solutions/> [Accessed: 15 August 2019]
- [17] Monemian E, Cairns A, Gilmore M, et al. Evaluation of intake charge hydrogen enrichment in a heavy-duty diesel engine. Proceeding of IMechE Part D: Journal of Automobile Engineering. 2017;232:139-147
- [18] Stenlås O, Christensen M, Egnell R, et al. Hydrogen as Homogeneous Charge Compression Ignition Engine Fuel. SAE Technical Paper 2004-01-1976. 2004
- [19] Rosati MF, Aleiferis PG. Hydrogen SI and HCCI Combustion in a Direct-

- Injection Optical Engine. SAE Technical Paper 2009-01-1921. 2009
- [20] Lanz A et al. Hydrogen Fuel Cell Engines and Related Technologies. CA, USA: College of the Desert; 2001
- [21] Cassidy JF. Emissions and Total Energy Consumption of a Multicylinder Piston Engine Running on Gasoline and a Hydrogen-Gasoline Mixture. Springfield, Virginia, USA: National Technical Information Service; 1977
- [22] Engine Performance Application Manual (v2018), Gamma Technologies. Westmont, IL, USA; 2018
- [23] Metghalchi M, Keck JC. Burning velocities of mixtures of air with methanol, iso-octane, and Indolene at high pressure and temperature. *Combustion and Flame*. 1982;48:191
- [24] Heywood JB. Internal Combustion Engine Fundamentals. 1st ed. New York, NY: McGraw-Hill; 1988
- [25] Blizzard NC, Keck JC. Experimental and Theoretical Investigation of a Turbulent Burning Model for Internal Combustion Engines. SAE Technical Paper 740191. 1974
- [26] Hires SD, Tabaczynski RJ, Novak JM. The Prediction of Ignition Delay and Combustion Intervals for a Homogeneous Charge, Spark Ignition Engine. SAE Technical Paper 780232. 1978
- [27] Walther H, Schlatter S, Wachtmeister G, Boulouchos K. Combustion Models for Lean-Burn Gas Engines with Pilot Injection, MTZ Paper 02I2012. 2011
- [28] Dhole AE, Yarasu RB, Lata DB. Investigations on the combustion duration and ignition delay period of a dual fuel diesel engine with hydrogen and producer gas as secondary fuels. *Applied Thermal Engineering*. 2016;107:524-532
- [29] Verhelsta S, Wallnerb T. Hydrogen-fueled internal combustion engines. *Progress in Energy and Combustion Science*. 2009;35(6):490-527. Available from: <https://biblio.ugent.be/publication/818298>